

Speciation of ferric phenoxide intermediates during the reduction of iron(III)- μ -oxo dimers by hydroquinone

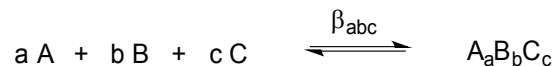
William D. Kerber, Kaitlyn A. Perez, Chuqiao Ren, and Maxime A. Siegler.

Supporting Information

Iron(III)-TPA stability constants.....	S2
Acidity of iron(III)-aquo complexes.....	S5
Kinetic data from the reaction of 1 with excess hydroquinone	S7
Absorbance vs time plots at pH 5.6	S7
Log plots at pH 5.6	S8
Log plots at pH 4.1-5.2	S9
Mechanism and rate law for reaction of 1 with hydroquinone.....	S10
Proposed mechanism.....	S10
Derivation of the complete rate law.....	S11
Simplified rate law at high pH limit.....	S14
Rate law at pH 5.6.....	S15
Reaction parameters.....	S15
Estimated upper limit of K_{2b}	S15
Summary	S17
Absorption spectra of iron(III)-TPA phenoxide complexes in acetonitrile	S18
Molar absorptivity of $[\text{Fe}(\text{TPA})(2\text{-naphtholate})(\text{OCH}_3)]\text{ClO}_4$ (6).....	S18
References	S20

Iron(III)-TPA stability constants

Throughout this work the term stability constant (β) is used to define the equilibrium constant associated with formation of a particular complex from its component parts:



Negative subscripts for protons refer to loss of H^+ from coordinated water molecules in the product. Because the equilibrium constants span many orders of magnitude they are reported on a log scale ($\log \beta_{abc}$). Concentrations are used instead of activities throughout, on the assumption that the quotient of activity factors remains constant in a medium of constant ionic strength. Glass electrodes were calibrated in terms of the hydrogen ion concentration at the same constant ionic strength. By convention, the concentration of water is taken to be constant and is ignored in all equilibrium calculations. For a general introduction to stability constants the reader is referred to the excellent text by Martell & Motekaitis.¹ The basis for the fitting algorithms used in Hyperquad is discussed in a monograph by Gans.² The work of Braibanti *et. al.* provides an experimental framework for practitioners of stability constant determination to test their apparatus and technique.³

The final refined speciation model for the iron(III)-TPA system is shown in Table S1; these data were used to generate a pH-dependent speciation diagram under the conditions investigated in this work (Figure S1). Note that the dominant species are from the TPA buffer, which have been omitted for clarity from Figure 1. The final model was refined using the twelve individual pH titrations listed in Table S2. The conditions of these experiments were designed to sample a range of concentrations and metal:ligand ratios. Parameters in bold were refined and all others were held constant. The values of TPA protonation constants were determined separately and are shown in Table S3; these values are in good agreement with other reports in the literature.⁴ Iron hydrolysis constants were taken from the literature;⁵ these species are not particularly important in the pH range investigated in this work (see Figure S1) but they were included in the model as constants for completeness. Hyperquad2008 provides an estimate of uncertainty in each refined parameter based on known experimental uncertainties. (titer volume $\pm 0.3\%$ and electrode potential ± 0.1 mV with the setup described in Experimental). These uncertainties are reported in parentheses in Table S2 and Table S3. The averages of the refined stability constants are reported in Table S1.

Table S1. Proposed speciation model for the aqueous iron(III)-TPA system.

Species	Formation constant	log β
$\text{Fe}[\text{TPA}]^{+3}(\text{aq})$	β_{110}	10.75(15) [†]
1a	β_{22-2}	19.91(12) [‡]
1b	β_{22-3}	15.53(6) [‡]
1c	β_{22-4}	10.27(7) [‡]
$(\text{TPA})\text{H}^+$	β_{011}	6.102(6) [†]
$(\text{TPA})\text{H}_2^{+2}$	β_{012}	10.398(12) [†]
$(\text{TPA})\text{H}_3^{+3}$	β_{013}	12.93(4) [†]
$[\text{Fe}(\text{H}_2\text{O})_5\text{OH}]^{+2}$	β_{10-1}	-2.54
$[\text{Fe}(\text{H}_2\text{O})_5(\text{OH})_2]^+$	β_{10-2}	-6.14
$[(\text{H}_2\text{O})_5\text{Fe}]_2\text{O}$	β_{20-2}	-2.79
OH^-	$\beta_{00-1} (K_w)$	-13.78

Average values from Tables S2 and S3 are reported here. [†] uncertainty given as standard deviation;

[‡]uncertainty given as standard error of the mean

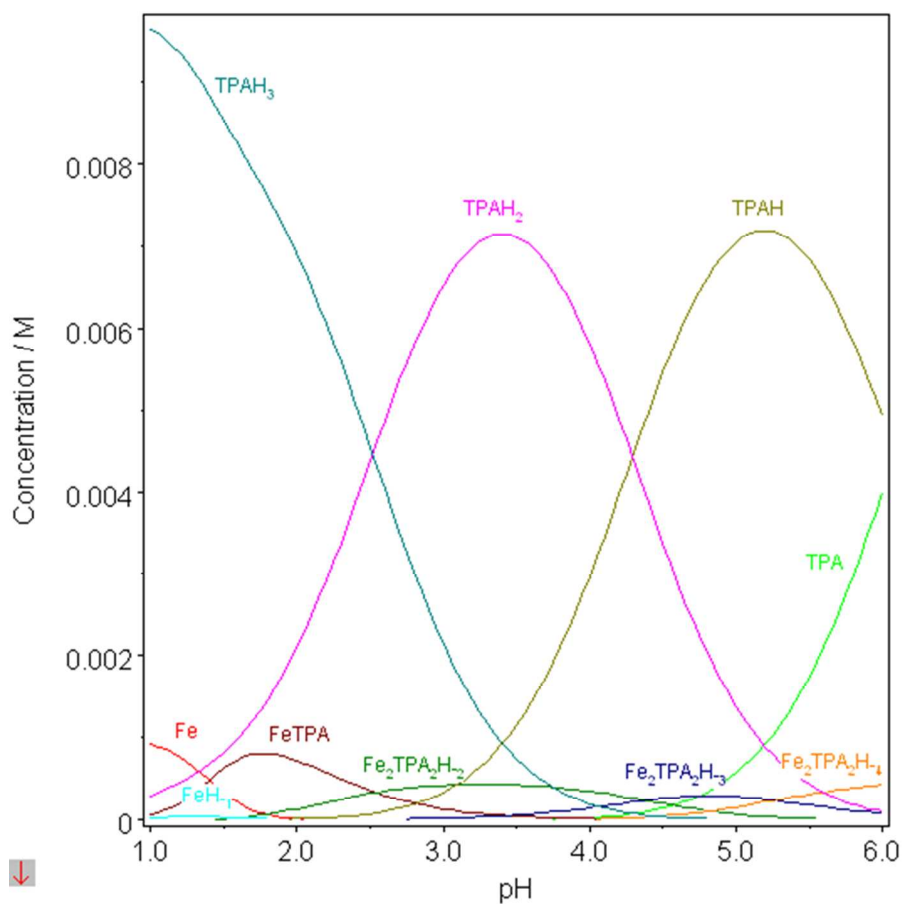


Figure S1. pH-dependent speciation diagram for a solution containing 1 mM Fe^{+3} and 10 mM TPA (25°C; $I = 0.100$ M) generated from the model in Table S1.

Table S2. Summary of iron(III)-TPA titration experiments. Stability constants in **bold** were refined; all others held constant.

<i>Experimental conditions*</i>				<i>iron(III)-TPA formation constants</i>				<i>TPA protonation constants</i>			<i>iron hydrolysis constants</i>			K_w
#	[Fe] mM	[TPA] mM	pH range	log β_{110}	log β_{22-1} (1a)	log β_{22-2} (1b)	log β_{22-3} (1c)	log β_{011}	log β_{012}	log β_{013}	log β_{10-1}	log β_{10-2}	log β_{20-2}	log β_{00-1}
1	0.197	0.588	5.4-2.1	10.71(10)	19.6(2)	15.2(2)	10.0(2)	6.102	10.398	12.930	-2.54	-6.14	-2.79	-13.78
2	0.197	0.588	5.4-2.1	10.63(7)	19.45(13)	15.08(13)	9.92(13)	6.102	10.398	12.930	-2.54	-6.14	-2.79	-13.78
3	0.197	0.588	5.4-2.1	10.91(12)	20.2(2)	15.8(2)	10.5(2)	6.102	10.398	12.930	-2.54	-6.14	-2.79	-13.78
4	1.002	7.98	5.6-2.1	10.75	20.09(7)	15.49(8)	9.79(9)	6.102	10.398	12.930	-2.54	-6.14	-2.79	-13.78
5	1.002	7.98	5.6-2.1	10.75	20.15(6)	15.64(6)	9.96(7)	6.102	10.398	12.930	-2.54	-6.14	-2.79	-13.78
6	0.196	0.781	5.4-2.1	10.75	20.02(5)	15.55(5)	10.38(5)	6.102	10.398	12.930	-2.54	-6.14	-2.79	-13.78
7	1.055	8.42	5.6-3.7	10.75	19.91	15.807(11)	10.366(11)	6.102	10.398	12.930	-2.54	-6.14	-2.79	-13.78
8	0.195	0.972	5.4-4.0	10.75	19.91	15.535(8)	10.333(6)	6.102	10.398	12.930	-2.54	-6.14	-2.79	-13.78
9	0.196	0.781	5.4-4.0	10.75	19.91	15.585(5)	10.387(4)	6.102	10.398	12.930	-2.54	-6.14	-2.79	-13.78
10	0.197	0.588	5.4-4.1	10.75	19.91	15.574(7)	10.35(5)	6.102	10.398	12.930	-2.54	-6.14	-2.79	-13.78
11	0.195	0.972	5.4-4.0	10.75	19.91	15.575(8)	10.436(6)	6.102	10.398	12.930	-2.54	-6.14	-2.79	-13.78
12	0.196	0.781	5.4-4.0	10.75	19.91	15.571(9)	10.437(6)	6.102	10.398	12.930	-2.54	-6.14	-2.79	-13.78

*Solutions adjusted to upper pH by addition of 0.1 N NaOH and then titrated down with 0.1 N HNO₃. No precipitated phases were detected in any titration. A minimum of 20 <mV,mL> data points per refined stability constant were collected with an equilibration time of 180 sec between points. Electrode calibration performed twice daily using the GLEE/vIpH method and raw mV data were converted to pH in Hyperquad2008 before refinement. T = 25.0±0.1°C and I = 0.100 (NaNO₃)

Table S3. Summary of TPA titration experiments. Stability constants in **bold** were refined; all others were held constant.

<i>Experimental conditions*</i>			<i>TPA protonation constants</i>			K_w
#	[TPA] mM	pH range	log β_{011}	log β_{012}	log β_{013}	log β_{00-1}
1	1.17	6.8-2.5	6.0978(9)	10.3842(12)	12.887(3)	-13.78
2	0.972	7.0-2.5	6.1044(18)	10.392(2)	12.912(5)	-13.78
3	1.36	6.8-2.6	6.110(1)	10.4126(13)	12.964(3)	-13.78
4	2.91	7.3-2.5	6.0964(8)	10.4031(11)	12.954(2)	-13.78

*Solutions adjusted to upper pH by addition of 0.1 N NaOH and then titrated down with 0.1 N HNO₃. A minimum of 20 <mV,mL> data points per refined stability constant were collected with an equilibration time of 30 sec between points. Electrode calibration performed twice daily using the GLEE method and raw mV data were converted to pH in Hyperquad2008 before refinement. T = 25.0±0.1°C and I = 0.100 (NaNO₃)

Acidity of iron(III)-aquo complexes

Acidity constants compiled from the literature for a variety of iron(III)-aquo complexes are presented in Table S4. Orbital arguments predict that the Lewis-assisted Brønsted acidity of the $\text{Fe}^{+3}\text{-OH}_2$ moiety should decrease when iron is coordinated by strong σ -donor ligands and increase when coordinated by π -acceptor ligands. The entries in Table S4 are divided into mononuclear iron(III) complexes, dinuclear iron(III) complexes, and iron(III) porphyrins; all entries show decreased acidity relative to $[\text{Fe}(\text{H}_2\text{O})_6]^{+3}$. The mononuclear iron(III) complexes generally contain bulky tetra-, penta-, or hexadentate ligands that inhibit μ -oxo dimer formation and these diverse ligand architectures serve to mask structural trends in the pK_a of the $\text{Fe}^{+3}\text{-OH}_2$ unit. Decreasing positive charge roughly correlates with increasing pK_a , and the only anionic complex in the group, $[\text{Fe}(\text{EDTA})(\text{H}_2\text{O})]^-$, is by far the weakest acid.

The dinuclear iron(III) complexes are a somewhat more homologous series. $[\text{Fe}_2(\mu\text{-O})(\text{phen})_4(\text{H}_2\text{O})_2]^{+4}$ and $[\text{Fe}_2(\mu\text{-O})(\text{TPA})_2(\text{H}_2\text{O})_2]^{+4}$ both contain $(\text{H}_2\text{O})\text{Fe-O-Fe}(\text{OH}_2)$ moieties capped with N_4 ligands. These tetracations have the largest positive charge in the series and consequently are the most acidic ($\text{pK}_{a1} \approx 4$). Their tricationic conjugate bases are less acidic by 0.9-1.6 log units. $[\text{Fe}_2(\text{BBPPNOL})(\mu\text{-OAc})(\text{H}_2\text{O})_2]^{+2}$ and $[\text{Fe}_2(\text{BPCINOL})_2(\text{H}_2\text{O})_2]^{+2}$ are dications owing to the presence of a phenoxide ligand in the coordination sphere of each iron. These *bis*-aquo complexes are less acidic than the tetracations with $\text{pK}_{a1} \approx 5$. Their monocationic conjugate bases are less acidic by 1.5-2 log units.

The first acidity constants of all six *meso*-substituted iron(III) porphyrins in Table S4 span 4 orders of magnitude even though all of the water ligands are all in essentially the same coordination environment. This again tracks with overall charge on the complex; water-soluble porphyrins generally have either cationic or anionic peripheral groups that solubilize the non-polar porphyrin and thus tune the acidity of the water molecules coordinated to iron(III).

Table S4. Acid dissociation constants for various iron(III)-aquo complexes^a

Complex ^b	pK _{a1}	pK _{a2}	Reference
[Fe(H ₂ O) ₆] ³⁺	2.54 ^c	3.60 ^c	5
<i>Mononuclear iron(III) complexes</i>			
[Fe(mpac)(H ₂ O) ₂] ⁺²	3.4	7.0	6
Fe(NTA)(H ₂ O) ₂	3.75	7.4	7
[FeCl(ImTASN)(H ₂ O)] ⁺²	3.8	--	8
[Fe(PY ₃ -py[14]aneN ₄)(H ₂ O)] ⁺³	4.11	--	9
[Fe(dpac)(H ₂ O)] ⁺²	5.2	--	6
[Fe(dapsox)(H ₂ O) ₂] ⁺	5.78	9.45	10
[Fe(EDTA)(H ₂ O)] ⁻	7.53	--	7
<i>Dinuclear iron(III) complexes</i>			
[Fe ₂ (μ-O)(phen) ₄ (H ₂ O) ₂] ⁺⁴	3.71	5.28	11
[Fe ₂ (μ-O)(TPA) ₂ (H ₂ O) ₂] ⁺⁴	4.38	5.26	This work
[Fe ₂ (BBPPNOL)(μ-OAc)(H ₂ O) ₂] ⁺²	4.88	6.33	12
[Fe ₂ (BPCINOL) ₂ (H ₂ O) ₂] ⁺²	5.0	7.0	13
<i>Iron(III) porphyrins</i>			
[Fe(TcatP)(H ₂ O) ₂] ⁺⁵	4.1	--	14
[Fe(TMpyP)(H ₂ O) ₂] ⁺⁵	5.79	11.71	15
[Fe(TMNP)(H ₂ O) ₂] ⁺⁵	6.09	10.28	15
[Fe(TCPS)(H ₂ O) ₂] ⁻⁴	6.72	9.58	16
[Fe(TPPS)(H ₂ O) ₂] ⁻³	7.0	--	17
[Fe(TanP)(H ₂ O) ₂] ⁻³	8.0	--	14

[a] Not corrected for temperature or ionic strength; [b] Ligand abbreviations: **Hmpac** = 2-[*N*-methyl-*N*-pyridin-2-ylmethyl]-amino-*N'*-quinolin-8-yl-acetamide]; **H₃NTA** = nitrilotriacetic acid; **ImTASN** = 4-((1-Methyl-1H-imidazol-2-yl)methyl)-1-thia-4,7-diazacyclononane; **PY₃-py[14]aneN₄** = 3,7,11-Tris(2-pyridylmethyl)-3,7,11,17-tetraazabicyclo-[11.3.1]heptadeca-1(17),13,15-triene; **Hdpac** = 2-[*N,N*-bis(pyridin-2-ylmethyl)]-amino-*N'*-quinolin-8-yl-acetamide; **H₂dapsox** = 2,6-diacetylpyridine-bis(semioxamazine); **H₄EDTA** = ethylenediaminetetraacetic acid; **phen** = 1,10-phenanthroline; **TPA** = *tris*(pyridylmethyl)amine; **H₃BBPPNOL** = *N,N'*-bis(2-pyridylmethyl)-*N,N'*-bis(2-hydroxybenzyl)-1,3-diaminopropan-2-ol; **H₄BPCINOL** = [*N*-2-hydroxybenzyl)-*N*-(pyridylmethyl)(3-chloro)(2-hydroxy)]propylamine]; **H₂TcatP** = 5 α ,10 β ,15 α ,20 β -tetrakis(2-(*N,N,N*-trimethylammoniumacetamido)phenyl)porphyrin; **H₂TMpyP** = 5,10,15,20-tetrakis(1-methylpyridinium-4-yl)porphyrin; **H₂TMNP** = 5 α ,10 β ,15 α ,20 β -tetrakis(2-(*N*-methylnicotinamido)phenyl)porphyrin; **H₂TCPS** = 5,10,15,20-tetrakis(4-carboxylatophenyl)porphyrinato; **H₂TPPS** = 5,10,15,20-tetrakis(4-sulfonatophenyl)porphyrin; **H₂TanP** = 5 α ,10 β ,15 α ,20 β -tetrakis(2-(sulfonatoacetamido)phenyl)porphyrin; **NAcMP8** = *N*-acetylated octapeptide from cytochrome c, *N*-acetylmicroperoxidase-8; [c] There is not general agreement in the literature as to the exact values of Fe(H₂O)₆⁺³ pK_{a1,2}; Representative values are shown here, see: Perrin, D. D. *Ionisation constants of inorganic acids and bases in aqueous solution*; 2nd ed.; Pergamon Press: Oxford, U.K., 1982, pp. 62-64.

Kinetic data from the reaction of **1** with excess hydroquinone

Absorbance vs time plots at pH 5.6

Representative kinetic data from the reaction of **1** with excess hydroquinone at pH 5.6 are shown in Figure S2. First-order rate constants were obtained by fitting a single exponential function; a minimum of four replicate trials were performed for each experiment.

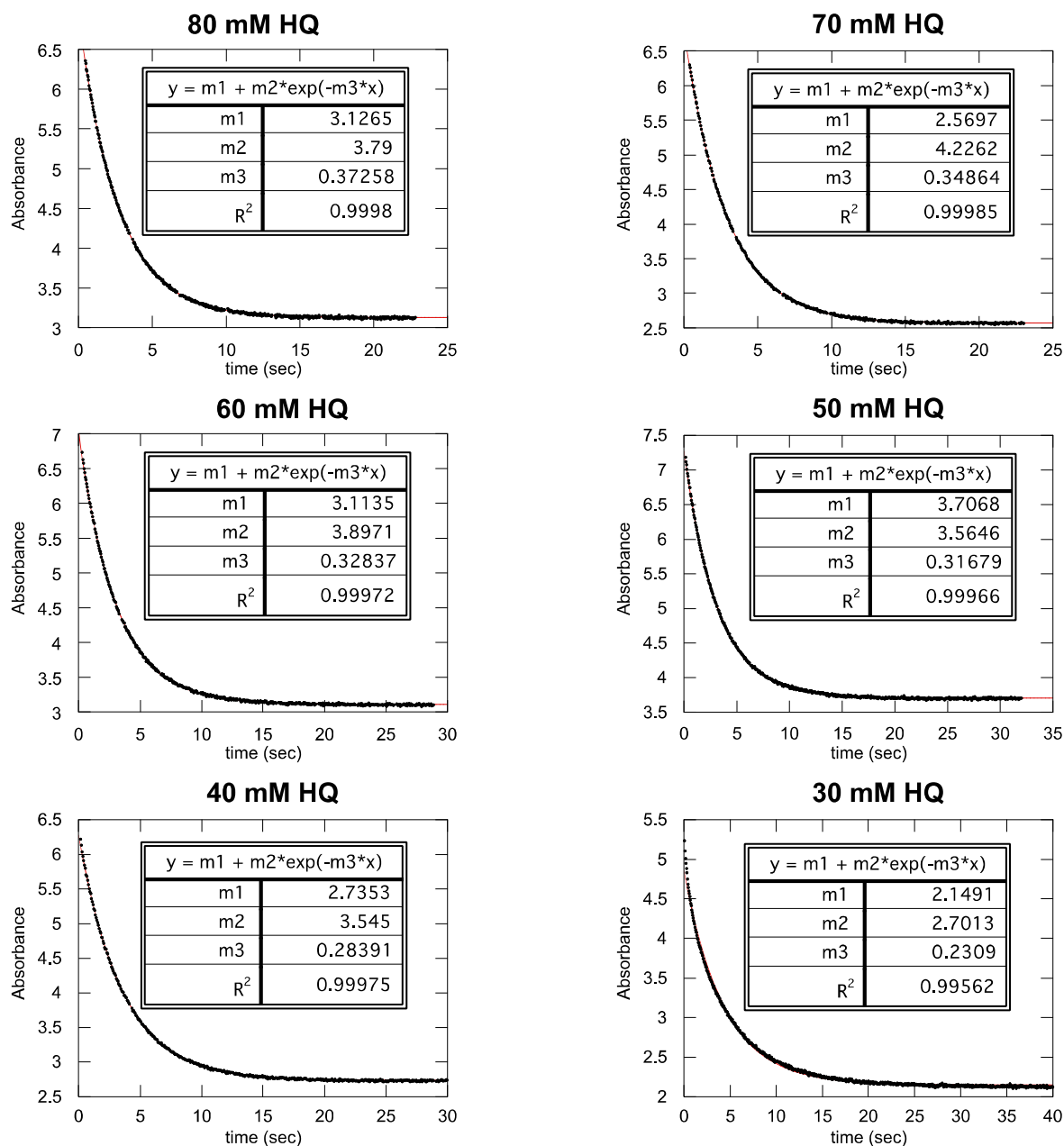


Figure S2. Integrated absorbance from 485-505 nm vs time for solutions of **1** reacting with excess hydroquinone. Conditions: $[\text{Fe}^{+3}]_0 = 1.0 \text{ mM}$; $[\text{TPA}] = 10 \text{ mM}$; $\text{pH} = 5.58 \pm 0.05$.

Log plots at pH 5.6

The linearity of log plots of absorbance vs time data was used to test the adherence of each experiment to a 1st order rate law. At pH 5.6, good 1st order behavior was observed when hydroquinone was held in large excess (Figure S3; $[HQ]_0 = 40 - 80 \text{ mM}$; 80 – 160 equivalents relative to **1**). Solubility constrained the practical upper limit of $[HQ]_0$ to at most 80 mM.¹⁸ Linearity of the log plots begins to degrade slightly at $[HQ] = 30 \text{ mM}$ and so this data point was not included in the pre-equilibrium binding plot in Figure 3; however, an observed 1st-order rate constant of c.a. 0.2 s^{-1} at 30 mM HQ is consistent with the non-linear dependence of k_{obs} on $[HQ]$.

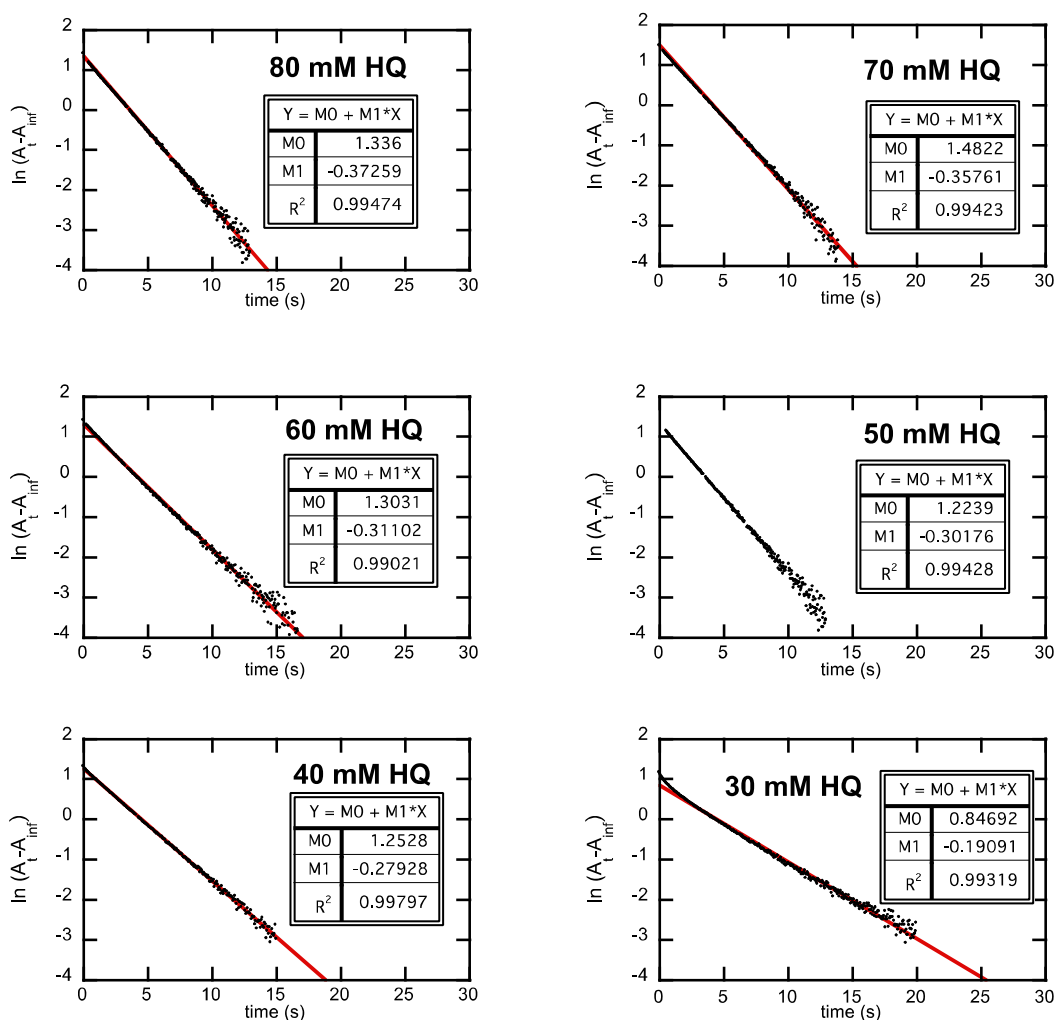


Figure S3. Log plots of integrated absorbance from 485-505 nm of solutions of **1** reacting with excess hydroquinone. Conditions: $[Fe^{+3}]_0 = 1.0 \text{ mM}$; $[TPA] = 10 \text{ mM}$; $\text{pH} = 5.58 \pm 0.05$.

Log plots at pH 4.1-5.2

At lower pH (4.07-5.16) log plots developed a distinct curvature consistent with a change in reaction mechanism. (Figure S4). Although an observed rate constant could not be obtained, the qualitative trend is decreasing reaction rate with decreasing pH.

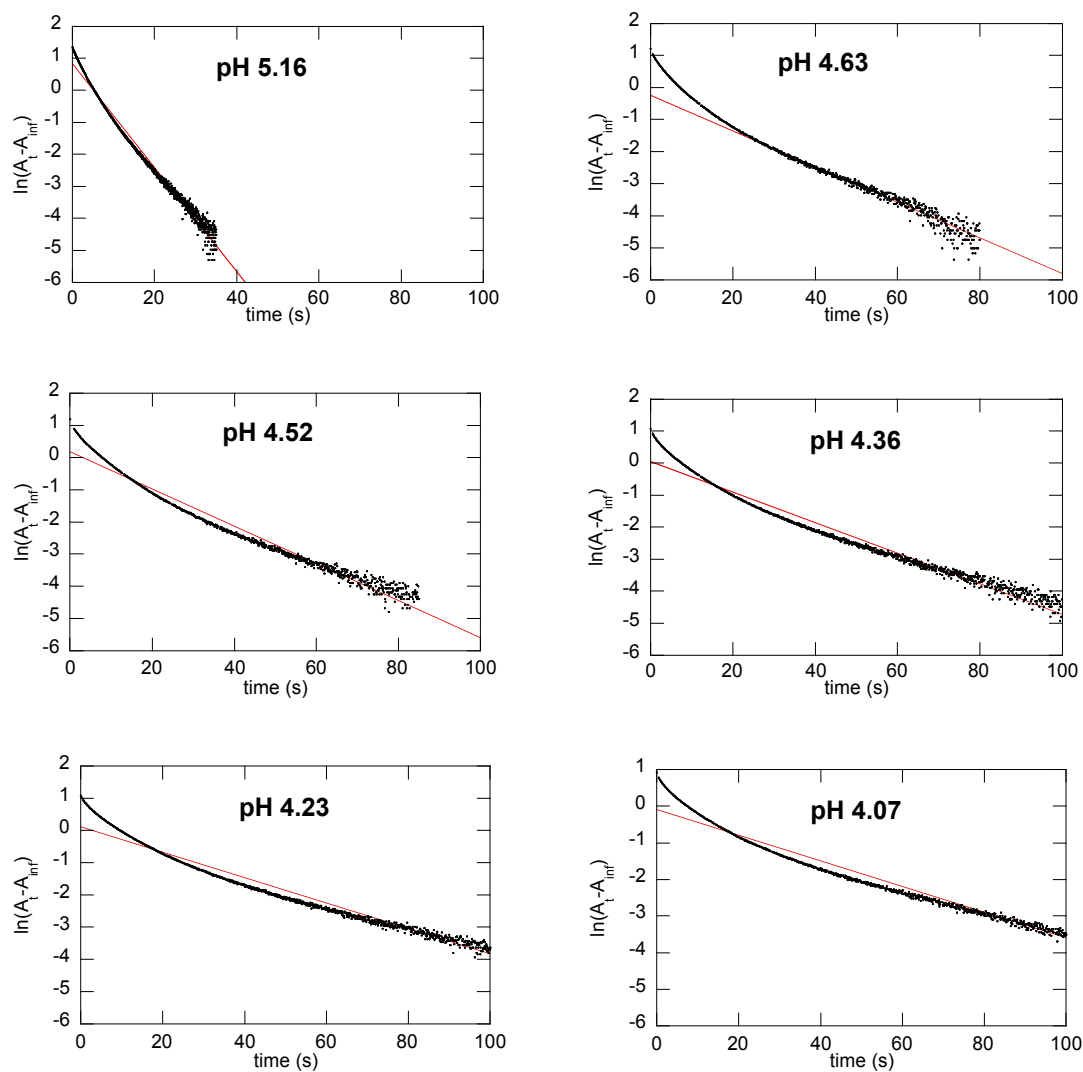
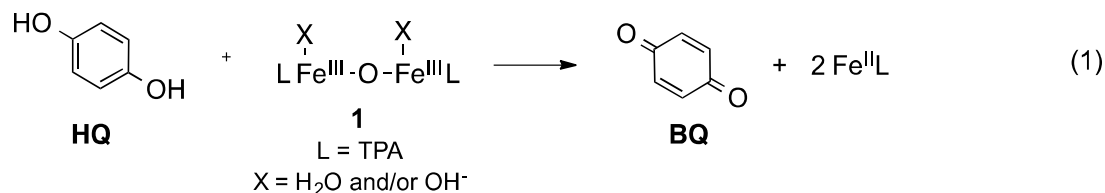


Figure S4. Log plots of integrated absorbance from 485-505 nm of solutions of **1** reacting with excess hydroquinone; Conditions: $[\text{Fe}^{+3}]_0 = 1.0 \text{ mM}$; $[\text{TPA}] = 10 \text{ mM}$; $[\text{HQ}]_0 = 60 \text{ mM}$.

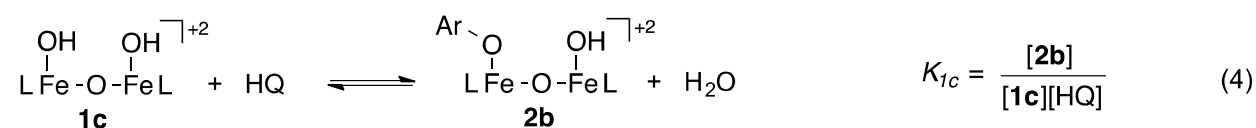
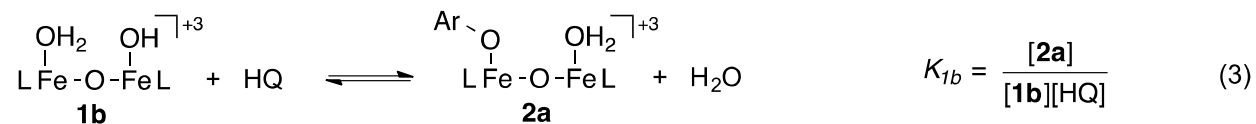
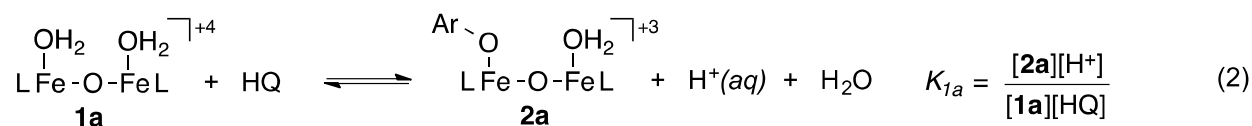
Mechanism and rate law for reaction of **1** with hydroquinone

Proposed mechanism

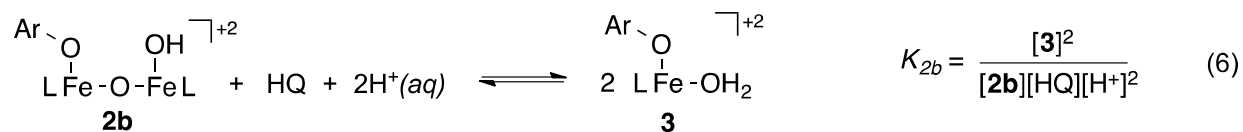
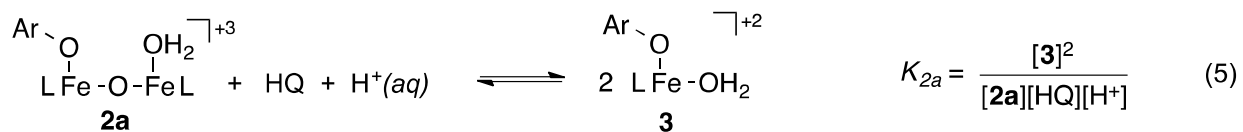
The experimentally determined stoichiometry for reaction of hydroquinone (HQ) with iron(III)-TPA dimer **1** is shown in Eq 1.



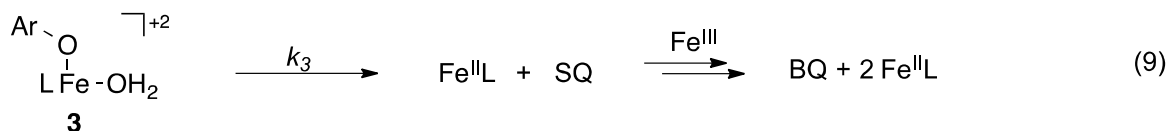
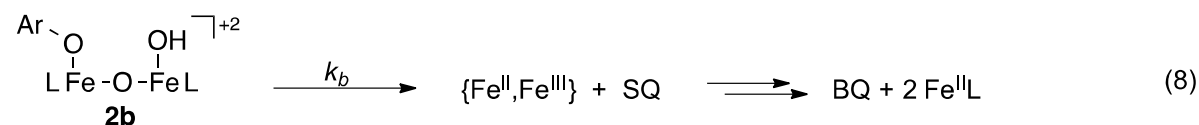
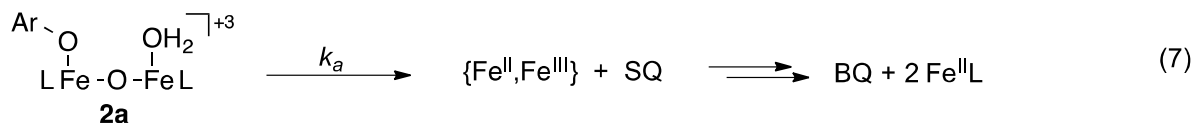
The proposed mechanism begins with substitution of a H₂O/OH⁻ ligand on **1** by HQ to form an iron(III)-phenoxide intermediate (**2**). Complex **1** has three protonation states (**a-c**) and complex **2** has two (**a-b**).¹⁹ The complete pH-dependent ligand substitution process is described by Eqs 2-4.



Coordination of a phenol to **1** promotes acidic cleavage of the μ -oxo dimer to form the mononuclear iron(III)-phenoxide **3**. This is included in the mechanistic scheme by adding Eqs 5-6. Only one protonation state of **3** is relevant because LFe^{III}(X)(OH) species favor formation of μ -oxo dimers; see discussion of [LFe(H₂O)(OH)]⁺ in the manuscript.



The rate-determining step is proposed to be inner-sphere electron transfer from HQ to iron(III) to release the semiquinone radical (SQ) from iron(II). This process is essentially irreversible because SQ will rapidly reduce another equivalent of iron(III) to give benzoquinone. Electron transfer is conceivable from any of the iron(III)-phenoxide intermediates, as shown in Eqs 7-9.



Derivation of the complete rate law

Because proton transfer and Fe^{+3} ligand substitutions are both fast processes, the assumption is made that Eqs 2-6 have reached equilibrium prior to rate-determining electron transfer. Mass-balance is achieved with Eqs 10-12²⁰ and the rate law for the reaction, expressed as the change in the total iron(III) concentration, is shown in Eq 13.

$$[\mathbf{1}] = [\mathbf{1a}] + [\mathbf{1b}] + [\mathbf{1c}] = \frac{[\mathbf{1c}]}{\alpha_{1c}} \quad (10)$$

$$[2] = [2a] + [2b] = \frac{[2b]}{\alpha_{2b}} \quad (11)$$

$$[\text{Fe}_T^{\text{III}}] = 2[1] + 2[2] + [3] = \frac{2[1c]}{\alpha_{1c}} + \frac{2[2b]}{\alpha_{2b}} + [3] \quad (12)$$

$$-\frac{1}{2} \frac{d[\text{Fe}_T^{\text{III}}]}{dt} = k_a[2a] + k_b[2b] + k_3[3] \quad (13)$$

The composite rate constant k' is a pH-weighted average of k_a and k_b (Eq 14). Substitution of k' into Eq 13 gives Eq 15.

$$k_a[2a] + k_b[2b] = (k_a\alpha_{2a} + k_b\alpha_{2b}) [2] = k'[2] \quad (14)$$

$$-\frac{1}{2} \frac{d[\text{Fe}_T^{\text{III}}]}{dt} = k'[2] + k_3[3] \quad (15)$$

The rate law in Eq 15 is rewritten in terms of $[2b]$ alone using the equilibrium expressions in Eqs 2-6 and mass-balance Eqs 10-11.

$$-\frac{1}{2} \frac{d[\text{Fe}_T^{\text{III}}]}{dt} = [2b] \left(\frac{k'}{\alpha_{2b}} + k_3[H^+] \sqrt{\frac{K_{2b}[HQ]}{[2b]}} \right) \quad (16)$$

Next, the concentration of $[2b]$ is solved for in terms total iron(III) concentration $[\text{Fe}_T^{\text{III}}]$ alone by substituting Eqs 4 and 6 in to Eq 12.

$$\begin{aligned} [\text{Fe}_T^{\text{III}}] &= \frac{2[2b]}{\alpha_{1c}K_{1c}[HQ]} + \frac{2[2b]}{\alpha_{2b}} + [H^+] \sqrt{K_{2b}[HQ][2b]} \\ &= \frac{2\alpha_{2b} + 2\alpha_{1c}K_{1c}[HQ]}{\alpha_{1c}K_{1c}[HQ]} [2b] + [H^+] \sqrt{K_{2b}[HQ]} \sqrt{[2b]} \quad (17) \end{aligned}$$

Eq 17 has the form

$$z = x[2b] + y\sqrt{[2b]} \quad (18)$$

where x and y are constant under the conditions of the reaction (excess HQ, constant pH)

$$z = [\text{Fe}_T^{\text{III}}]$$

$$x = \frac{2\alpha_{2b} + 2\alpha_{1c}K_{1c}[\text{HQ}]}{\alpha_{1c}\alpha_{2b}K_{1c}[\text{HQ}]}$$

$$y = [\text{H}^+]\sqrt{K_{2b}[\text{HQ}]}$$

Rearranging and squaring Eq 18 gives the polynomial

$$x^2[\mathbf{2b}]^2 - (2xz + y^2)[\mathbf{2b}] + z^2 = 0 \quad (19)$$

which has the solution²¹

$$[\mathbf{2b}] = \frac{(2xz + y^2) - \sqrt{y^2(y^2 + 4xz)}}{2x^2} \quad (20)$$

Substitution of Eq 20 into Eq 16 gives a rate law for the reaction in terms of the measurable value $[\text{Fe}_T^{\text{III}}]$ however its form is quite complex and the order in $[\text{Fe}_T^{\text{III}}]$ is fractional. 1st-order kinetics are not expected under any conditions without additional simplification.

Simplified rate law at high pH limit

Formation of the mononuclear complex **3** from **2** consumes protons (Eq 5-6), and at a high enough pH the concentration of **3** will decrease to the point that its term in Eq 12 will vanish. The expression for $[\text{Fe}_T^{\text{III}}]$ in terms of **2b** then takes on a much simpler form:

$$[\text{Fe}_T^{\text{III}}] = \frac{2[\mathbf{2b}]}{\alpha_{1c}K_{1c}[\text{HQ}]} + \frac{2[\mathbf{2b}]}{\alpha_{2b}} \quad (21)$$

which rearranges to

$$[\mathbf{2b}] = \frac{1}{2} \frac{\alpha_{1c}K_{1c}[\text{HQ}][\text{Fe}_T^{\text{III}}]}{1 + \frac{\alpha_{1c}}{\alpha_{2b}}K_{1c}[\text{HQ}]} \quad (22)$$

The rate law in Eq 16 can now be re-written by substituting in Eq 22 to show a first-order dependence on $[\text{Fe}_T^{\text{III}}]$ and simple Michaelis Menten-type saturation binding of HQ.²²

$$-\frac{d[\text{Fe}_T^{\text{III}}]}{dt} = \frac{k' \frac{\alpha_{1c}}{\alpha_{2b}} K_{1c}[\text{HQ}]}{1 + \frac{\alpha_{1c}}{\alpha_{2b}} K_{1c}[\text{HQ}]} [\text{Fe}_T^{\text{III}}] = k_{\text{obs}}[\text{Fe}_T^{\text{III}}] \quad (23)$$

When [HQ] is large and constant the overall reaction is first order and Beers law may be used to recast the integrated form of Eq 23 in terms of the total absorbance of all iron species at 495 nm (HQ and BQ are transparent at this wavelength). k_{obs} is evaluated from an exponential fit of Eq 24 to Abs_t vs time data.

$$\text{Abs}_t = (\text{Abs}_o - \text{Abs}_\infty)e^{-k_{\text{obs}}t} + \text{Abs}_\infty \quad (24)$$

Rate law at pH 5.6

The reaction of **1** with hydroquinone is not first order in $[\text{Fe}_T^{\text{III}}]$ from pH 4.1-5.2 but it becomes first order at pH 5.6. This means **[3]** is non-negligible at low pH but approaches zero as the pH approaches 5.6. As discussed below, these constraints may be used to provide an estimate of K_{2b} , the equilibrium constant that controls the concentration of **3**.

Reaction parameters

Most of the reaction parameters in the first-order regime are known or can be reliably estimated. The following values are known:

$$\begin{aligned}[\text{Fe}_T^{\text{III}}]_0 &= 9.9 \times 10^{-4} \text{ M} \\ [\text{HQ}] &= 0.060 \text{ M} \quad (\text{or another value in the range } 0.04 - 0.08 \text{ M}) \\ [\text{H}^+] &= 2.6 \times 10^{-6} \text{ M}\end{aligned}$$

The mole fraction α_{1c} is calculated from the speciation model in Table S1 at pH 5.58 using the software Hyss2009. The mole fraction α_{2b} is determined by the $\text{p}K_a$ of **2a** which is estimated to be 5.3 based on the acidity of other tricationic iron(III)- μ -oxo dimers given in Table S4.

$$\begin{aligned}\alpha_{1c} &= 0.66 \\ \alpha_{2b} &= \frac{K_{a(2a)}}{K_{a(2a)} + [\text{H}^+]} = 0.67\end{aligned}$$

K_{1c} is determined from the plot of k_{obs} vs $[\text{HQ}]$ in Figure 4 where $K_{1c}(\alpha_{1c}/\alpha_{2b}) = 25(3) \text{ M}^{-1}$ ($\alpha_{1c}/\alpha_{2b} = 0.99$).

$$K_{1c} = 25 \text{ M}^{-1}$$

Estimated upper limit of K_{2b}

For **[2b]** to have the linear dependence on $[\text{Fe}_T^{\text{III}}]$ shown in Eq 22, the magnitude of K_{2b} (Eq 6) must be small enough to produce a negligible amount of **3** at pH 5.6. If $K_{2b} \leq 1 \times 10^6 \text{ M}^{-2}$ then Eq 20 simplifies to Eq 25 as the $4xy$ term is at least 5×10^4 times greater than the y^2 term. Slightly higher values of K_{2b} would also be acceptable here but for reasons described below 10^6 is the upper limit.²³

$$[\mathbf{2b}] = \frac{(2xz + y^2) - \sqrt{y^2(4xz)}}{2x^2} = \frac{1}{x} \left(z + \frac{1}{2} \frac{y^2}{x} - y \sqrt{\frac{z}{x}} \right) \quad (25)$$

Eq 25 may be further simplified if the first term (z) dominates, which will occur if inequality 26 is satisfied. This occurs if $K_{2b} \leq 1 \times 10^6 \text{ M}^{-2}$, in which case Eq 25 becomes Eq 27 (which is also equal to Eq 22) and simple Michaelis-Menten saturation kinetics are predicted.

$$z \geq 100 \times \left[\frac{1}{2} \frac{y^2}{x} - y \sqrt{\frac{z}{x}} \right] \quad (26)$$

$$[\mathbf{2b}] = \frac{z}{x} = \frac{1}{2} \frac{\alpha_{1c} \alpha_{2b} K_{1c} [\text{HQ}]}{\alpha_{2b} + \alpha_{1c} K_{1c} [\text{HQ}]} [\text{Fe}_{\text{T}}^{\text{III}}] \quad (27)$$

The factor of 100 in Eq 26 was chosen somewhat arbitrary, but it provides an order-of-magnitude estimate for the maximum allowed value of K_{2b} that will give a linear relationship between $[\mathbf{2b}]$ and $[\text{Fe}_{\text{T}}^{\text{III}}]$ at pH 5.6.

Is $1 \times 10^6 \text{ M}^{-2}$ a reasonable estimate for K_{2b} ? This question may be addressed by considering the implications for iron(III) speciation as shown in Figure S5. Concentrations of iron(III) complexes were calculated in Hyss2009 using the data in Table S1, $\text{p}K_{\text{a}(\text{HQ})} = 9.9$, $\text{p}K_{\text{a}(2\text{a})} = 5.3$, $K_{1c} = 25 \text{ M}^{-1}$ and $K_{2b} = 10^6 \text{ M}^{-2}$.²⁴ At pH 5.58 complex **3** represents a negligible amount (0.9%) of $\text{Fe}_{\text{T}}^{\text{III}}$ but the concentration begins to rise quickly at pH decreases. This is consistent with the spectrophotometric titration of **1**/phenol shown in Figure 6. Although 10^6 is an upper limit for K_{2b} , the true value is likely to be within an order of magnitude because $K_{2b} \leq 10^5$ produces a negligible amount of **3** at any pH.²⁵

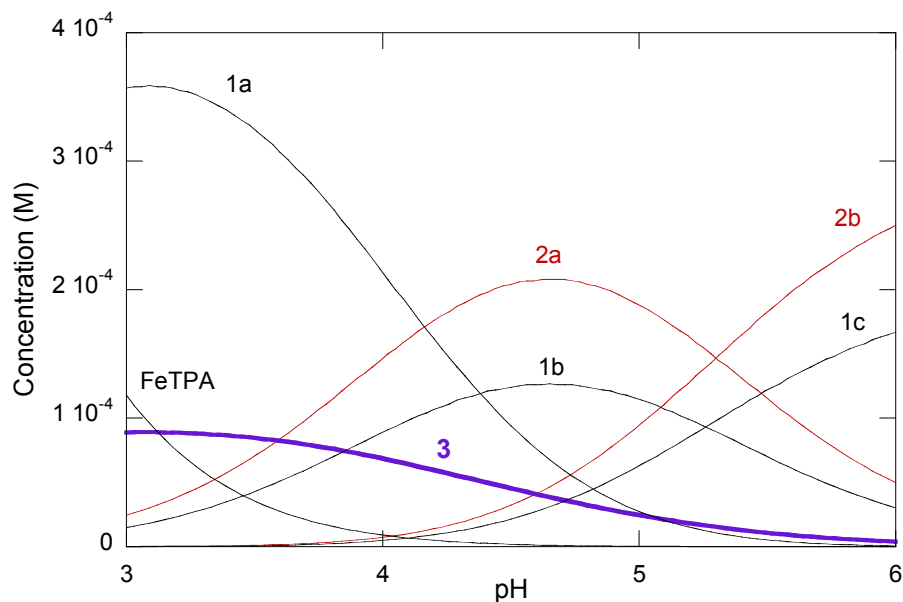


Figure S5. pH-dependent speciation of the iron(III)-TPA-HQ system shown at the upper limit of $K_{2b} = 1 \times 10^6 \text{ M}^{-2}$. Conditions: 1.0 mM Fe^{+3} ; 10.0 mM TPA; 60 mM HQ.

Summary

Inclusion of complex **3** in the proposed reaction mechanism for the oxidation of HQ by **1** leads to a rate law with a fractional order in $[\text{Fe}_T^{\text{III}}]$ because the iron(III) pool is partitioned between dimeric (**2**) and monomeric (**3**) species. The concentration of **3** decreases with increasing pH because its formation consumes protons and so there must be an upper pH limit after which the rate law reduces to a simple Michaelis Menten-type saturation binding regime. Kinetic data on the reaction at $[\text{Fe}_T^{\text{III}}]_0 = 1 \text{ mM}$ and $[\text{HQ}] = 40\text{-}80 \text{ mM}$ show first-order behavior at pH 5.58 but not below. If K_{2d} is $1 \times 10^6 \text{ M}^{-2}$ or slightly lower the concentration of **3** is negligible at pH 5.58 but becomes significant as the pH decreases.

Absorption spectra of iron(III)-TPA phenoxide complexes in acetonitrile

Addition of one equivalent of triethylamine to an iron(III)-TPA solution in acetonitrile with excess phenol gives a purple solution with $\lambda_{\text{max}} = 576 \text{ nm}$ (Figure S6). Continued addition of triethylamine increases the intensity of this band and gradually shifts it to 480 nm until 2.5 molar equivalents relative to iron have been added. This is the same behavior observed for the analogous titration in water (Figure 6) in which a pH 6.76 solution of **1** + phenol has a band at 471 nm that shifts to 570 nm with a concomitant decrease in intensity as the pH is lowered to 3.26.

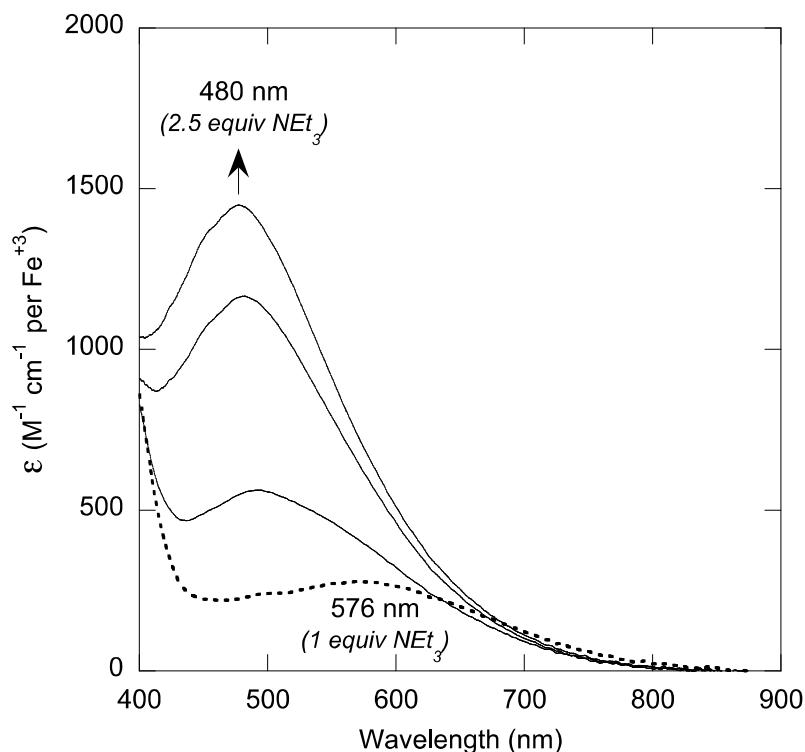


Figure S6. Titration of an iron(III)-TPA phenoxide complex with triethylamine in acetonitrile. Initial conditions (dashed line): 3.84 mM $\text{Fe}(\text{NO}_3)_3$, 3.88 mM TPA, 38.5 mM phenol, 3.84 mM triethylamine. Each subsequent spectrum represents addition of 0.5 molar equivalents of triethylamine relative to Fe^{+3} . No additional change was observed with greater than 2.5 equivalents of triethylamine

Molar absorptivity of $[\text{Fe}(\text{TPA})(2\text{-naphtholate})(\text{OCH}_3)]\text{ClO}_4$ (**6**)

Single crystals of **6** for X-ray diffraction were grown from a 10 mM methanol solution. To confirm that the solid-state structure of **6** matched the species formed *in situ*, a series of absorption spectra were

recorded. These are shown, corrected for molar absorptivity per Fe^{+3} in Figure S7 A. The dashed line is the *in situ* methanol solution and the solid line is isolated **6** re-dissolved in CH_2Cl_2 . The spectral profiles are similar except for a 5-fold increase in apparent molar absorptivity in CH_2Cl_2 . In aqueous solution iron(III)-TPA complexes are only partially coordinated by phenol, even when phenol is present in a large excess (see Figure 6 and associated discussion). The same behavior is observed in methanol. Addition of excess 2-naphthol to the methanol solution in Figure S7 A increases the intensity of the band at 562 nm. A plot of A_{562} vs $[\text{Fe}^{+3}]$ obtained by serial dilution of the methanol solution is non-linear. These data indicate partial equilibrium binding of 2-naphthol to iron(III)-TPA in methanol. In contrast, a plot A_{540} vs $[\mathbf{6}]$ from serial dilution of a CH_2Cl_2 solution is linear (Figure S7 B; $\epsilon_{540} = 1800 \text{ M}^{-1}\text{cm}^{-1}$). The absence of competitive ligand exchange with solvent in CH_2Cl_2 allows measurement of the true molar absorptivity of **6**.

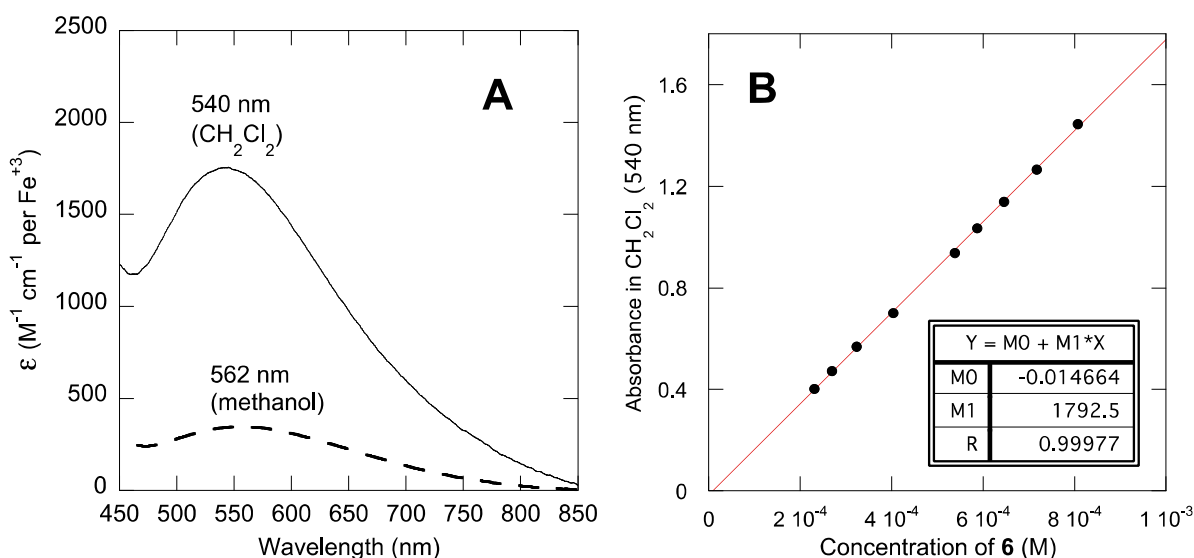


Figure S7. (A) Absorption spectra of isolated **6** in CH_2Cl_2 (solid line) and the *in situ* product generated from equimolar amounts of Fe^{+3} , TPA, and 2-naphthol in methanol (dashed line). (B) Molar absorptivity of **6** at 540 nm in CH_2Cl_2 determined to be $1800 \text{ M}^{-1}\text{cm}^{-1}$ from serial dilution of a 0.81 mM solution.

References

- (1) Martell, A. E.; Motekaitis, R. J. *Determination and Use of Stability Constants*; John Wiley & Sons: New York, 1992.
- (2) Gans, P. *Data Fitting in the Chemical Sciences*; John Wiley & Sons: Chichester, U.K., 1992.
- (3) Braibanti, A.; Ostacoli, G.; Paoletti, P.; Pettit, L. D.; Sammartano, S. *Pure Appl. Chem.* **1987**, *59*, 1721–1728.
- (4) Ambundo, E. A.; Deydier, M.-V.; Grall, A. J.; Aguera-Vega, N.; Dressel, L. T.; Cooper, T. H.; Heeg, M. J.; Ochrymowycz, L. A.; Rorabacher, D. B. *Inorg. Chem.* **1999**, *38*, 4233–4242.
- (5) R. H. Byrne, W. Yao, Y. Luo, B. Wang, *Marine Chem.*, **2005**, *97*, 34-48; P. Djurdjević, M. J. Stankov, J. Odović, *Polyhedron*, **2000**, *19*, 1085-1096.
- (6) Hitomi, Y.; Hiramatsu, K.; Arakawa, K.; Takeyasu, T.; Hata, M.; Kodera, M. *Dalton Trans.* **2013**, *42*, 12878-12882.
- (7) Delgado, R.; do Carmo Figueira, M.; Quintino, S. *Talanta* **1997**, *45*, 451–462.
- (8) Cui, J.; Mashuta, M. S.; Buchanan, R. M.; Grapperhaus, C. A. *Inorg. Chem.* **2010**, *49*, 10427–10435.
- (9) Costa, J.; Delgado, R.; Drew, M. G. B.; Félix, V. *J. Chem. Soc., Dalton Trans.* **1999**, 4331–4339.
- (10) Ivanovic-Burmazovic, I.; Hamza, M. S. A.; van Eldik, R. *Inorg. Chem.* **2002**, *41*, 5150–5161.
- (11) Bhattacharyya, J.; Dutta, K.; Mukhopadhyay, S. *Dalton Trans.* **2004**, 2910–2917.
- (12) Longhinotti, E.; Domingos, J. B.; Szpoganicz, B.; Neves, A.; Nome, F. *Inorg. Chim. Acta* **2005**, *358*, 2089–2092.
- (13) Neves, A.; Terenzi, H.; Horner, R.; Horn, A., Jr; Szpoganicz, B.; Sugai, J. *Inorg. Chem. Comm.* **2001**, *4*, 388–391.
- (14) Imai, H.; Yamashita, Y.; Nakagawa, S.; Munakata, H.; Uemori, Y. *Inorg. Chim. Acta* **2004**, *357*, 2503–2509.
- (15) G.M. Miskelly, W.S. Webley, C.R. Clark, D.A. Buckingham, *Inorg. Chem.* **1988**, *27*, 3773-3781.
- (16) J.D. Strong, C.R. Hartzell, *Bioinorg. Chem.* **1976**, *5*, 219-233.
- (17) A.D. El-Awady, P.C. Wilkins, R.G. Wilkins, *Inorg. Chem.* **1985**, *24*, 2053-2057.
- (18) A 1:1 mixing ratio of FeTPA and HQ requires 2x concentration of stock solutions and 160 mM is approaching the solubility limit of hydroquinone when NaNO₃ is added to maintain ionic strength.
- (19) Coordination to Fe⁺³ results in complete ionization of the phenol, hence Eqs 2 and 3 produce the same product **2a**, and $\log K_{1b} = \log K_{1a} + pK_{a1}$, see: (a) Desai, A. G.; Milburn, R. M. *J. Am. Chem. Soc.* **1969**, *91*, 1958–1961; (b) McBryde, W. *Can. J. Chem.* **1968**, *46*, 2385–2392.
- (20) The mole fraction of protonation state *x* is expressed as α_x and is constant at constant pH. Note that, for example, α_{1c} represents the fraction of **1** in protonation state **c**, *not* the fraction of total iron in complex **1c**.
- (21) The (+) solution to Eq 20 returns an invalid solution to Eq 18 when *x*, *y*, are *z* are positive numbers.
- (22) The *k*₃ term is dropped from Eq 16 because [**3**] approaches zero.

(23) On the other hand, Eq 20 would also have a linear dependence on $[\text{Fe}_T^{\text{III}}]$ at very large values of K_{2b} ($y^2 \gg 4ab$ when $K_{2b} \geq 10^{13} \text{ M}^{-2}$) but this means essentially 100% of Fe^{III} exists as the mononuclear complex **3** at pH 5.6. From the spectrophotometric titration of **1** with phenol shown in Figure 6 this is clearly not the case.

(24) Strictly speaking Hyss2009 accepts formation constants as inputs; β_{2a} , β_{2b} , and β_3 are easily calculated from the stepwise constants provided here and the data in Table S1.

(25) Reproducing Figure S4 with $K_{2b} = 10^5 \text{ M}^{-2}$ predicts $[\mathbf{3}] = 2 \times 10^{-5} \text{ M}$ at pH 4 (2% of Fe_T^{III}). This is probably too low given the **1**/phenol titration data.